

**Stochastic Optimization of Hydroelectric Dam Operations on the Biobío River  
in Chile**

by

Kristen M. Burrall

B.S., Environmental Engineering  
Massachusetts Institute of Technology, 2008

Submitted to the Department of Civil and Environmental Engineering in Partial Fulfillment of the  
Requirements for the Degree of

**Master of Engineering in Civil and Environmental Engineering**

at the  
**Massachusetts Institute of Technology**

June 2009

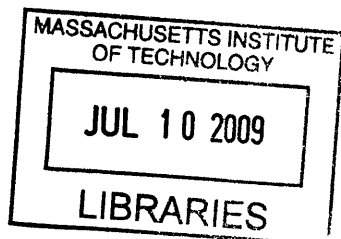
© 2009 Kristen M. Burrall  
All rights reserved

The author hereby grants to MIT permission to reproduce and to distribute publicly paper and  
electronic copies of this thesis document in whole or in part in any medium now known or hereafter  
created.

Signature of Author \_\_\_\_\_  
Department of Civil and Environmental Engineering  
May 8, 2009

Certified by \_\_\_\_\_  
Dennis B. McLaughlin  
H.M. King Bhumibol Professor of Water Resource Management  
Thesis Supervisor

Accepted by \_\_\_\_\_  
Daniele Veneziano  
Chairman, Departmental Committee for Graduate Students



**ARCHIVES**

# **Stochastic Optimization of Hydroelectric Dam Operations on the Biobío River in Chile**

by

Kristen M. Burrall

B.S., Environmental Engineering  
Massachusetts Institute of Technology, 2008

Submitted to the Department of Civil and Environmental Engineering on May 8, 2009 in partial fulfillment of the requirements for the Degree of Master of Engineering in Civil and Environmental Engineering

## **ABSTRACT**

Growing electricity demand in Chile has prompted the proposal of new hydropower projects. In addition to evaluating new projects to satisfy demand, a holistic assessment of alternatives as well as potential gains from improved utilization of current hydropower resources should be completed. This study aims to quantify potential gains from optimizing reservoir operations through a case study of the 2-dam system, consisting of the Pangué and Ralco dams, on the Biobío River. This analysis includes results from an optimization model built in GAMS (General Algebraic Modeling System) and two simulations built in MATLAB by the author to assess the efficacy of various operational schemes.

Thesis Supervisor: Dennis B. McLaughlin

Title: H.M. King Bhumibol Professor of Water Resource Management

## **ACKNOWLEDGEMENTS**

I owe my deepest gratitude to everyone involved in the Aysén dam debates who graciously offered advice, information, and perspective to our research team. I would especially like to thank Jonathan Leidich and Patagonia Adventure Expeditions for the insight and enthusiasm that helped us to better understand the physical and cultural environment in Aysén. I would also like to thank all other agencies, groups, and persons who communicated with us to offer data and guidance. This work is dedicated to Yoani Arratia, a vital guide and companion throughout our adventures.

## TABLE OF CONTENTS

<b>Abstract</b>	<b>2</b>
<b>Acknowledgements</b>	<b>3</b>
<b>1. Background</b>	<b>6</b>
<i>1.1. Energy in Chile</i>	<i>6</i>
<i>1.2. Motivation for Optimizing Reservoir Operations</i>	<i>6</i>
<b>2. Optimization Model</b>	<b>7</b>
<i>2.1. Model Overview</i>	<i>7</i>
<i>2.2. Data Analysis and Replicate Creation</i>	<i>8</i>
<i>2.3. Optimization Problem Formulation</i>	<i>9</i>
<b>3. Results</b>	<b>12</b>
<i>3.1. 6-Year Simulation</i>	<i>12</i>
<i>3.2. Replicate Simulation</i>	<i>15</i>
<i>3.3. Conclusions</i>	<i>15</i>
<b>Appendix A. Methods Detail</b>	<b>18</b>
<b>Appendix B. Assumptions</b>	<b>21</b>
<b>Appendix C. Literature Review</b>	<b>24</b>
<b>Appendix D. References</b>	<b>30</b>

## TABLE OF FIGURES

Figure 1: Ralco and Pangué Dams and Reservoirs (Ediciones Especiales, 2009)	7
Figure 2: Satellite Image of Biobío Basin	8
Figure 3: Schematic of Biobío Basin	9
Figure 4: Reservoir Flows, Current scenario	13
Figure 5: Reservoir Storage, Current scenario	13
Figure 6: Reservoir Flows, Optimal scenario	14
Figure 7: Reservoir Storage, Optimal scenario	14
Figure 8: Historical Data and Synthesized Time-Series for Ralco Inflow	19
Figure 9: Historical Data and Synthesized Time-Series for Trib2	19
Figure 10: Approximated Rainfall on the Ralco reservoir	22
Figure 11: Model Predictive Control Schematic (Nikolaou, 2001)	29

## 1. BACKGROUND<sup>1</sup>

### 1.1. Energy in Chile

Electricity demand in Chile centers on Santiago and the nation's mining industries (Pabich, 2008). Increased GDP and transport in Chile have heightened energy demand especially in the northern region. Chile aims to incorporate new energy at a rate of 400 to 700 Megawatts per year (CONAMA, 2009). Power needs are prompting the proposal of new hydropower projects, primarily HidroAysén's proposed dams on the Baker and Pascua rivers in the Aysén region, 1,400 miles south of Santiago. In light of the energy situation, it is prudent to consider a holistic assessment of both alternatives and potential for improving utilization of current resources, especially those closest to areas of concentrated demand.

This study aims to estimate potential gains from improved utilization of operational hydropower facilities in Chile. A case study of the two-dam system on the Biobío River was completed and results extrapolated to other systems. The Biobío system, consisting of dams Ralco and Pangué, is already connected to the Santiago grid (Sistema Interconectado Central, SIC) and thus any additional power obtained from the system should come at no additional cost or environmental damage.

### 1.2. Motivation for Optimizing Reservoir Operations

Chile has several multi-dam operations on its many large rivers. Dams are often placed in series on a single river, or on various tributaries within the same watershed. Since inflows to downstream dams are dependent on the releases from upstream dams, it is important to evaluate an operation scheme that considers these relationships, formulating a global watershed strategy that maximizes power output over all connected reservoirs.

On the Biobío River, the Ralco and Pangué dams and associated reservoirs are in series. The outflow from the upstream Ralco reservoir is a large component of the inflow to the Pangué reservoir (see Figure 1). The uncertainty of future hydrologic conditions must be considered. The most important uncertain inputs to the system include upstream and tributary flows, evaporative losses, and precipitation. This analysis describes an optimal operation plan that accounts for the interaction between reservoir releases while characterizing the most important unknown future inputs by analyzing historical variability.

---

<sup>1</sup> Components of this section are a result of a group effort between Kristen Burrall, Gianna Leandro, Laura Mar, Elisabetta Natale, and Flavia Tauro.



**Figure 1: Ralco and Pangué Dams and Reservoirs** (Ediciones Especiales, 2009)

Figure 1 displays the geographic relationship of the dams to each other as well as to the rest of the Biobío watershed. The river originates in the Andes Mountains and flows to the mouth at Concepción. The Río Laja, a tributary of the Biobío, is another important river for hydropower and can be seen in the graphic. The enlarged image shows the reservoirs (embalses), dams (presas), and the Ralco power station (Central Ralco). The túnel de aducción is the 7-kilometer pipe that takes water from the Ralco reservoir to the turbines.

## 2. OPTIMIZATION MODEL

### 2.1. Model Overview

This optimization used 30 synthetic flow series, called replicates, for each of two parameters. Each replicate consists of one year of monthly flows. The parameters modeled were aggregated inflow to the Ralco reservoir and tributary flow between the two reservoirs. The tributary flow between the reservoirs adds to the Ralco discharge to form the inflow to the Pangué reservoir. Considering each of the 30 replicates to be equally probable, the model maximizes expected total power, an average over each replicate of the sum of power produced at both dams over all time steps.

## 2.2. Data Analysis and Replicate Creation

Six years of daily flow data (2003-2009) were obtained from Dirección General de Aguas (DGA) flow stations (DGA, 2009). Flow stations and dam locations are noted in the satellite image below.

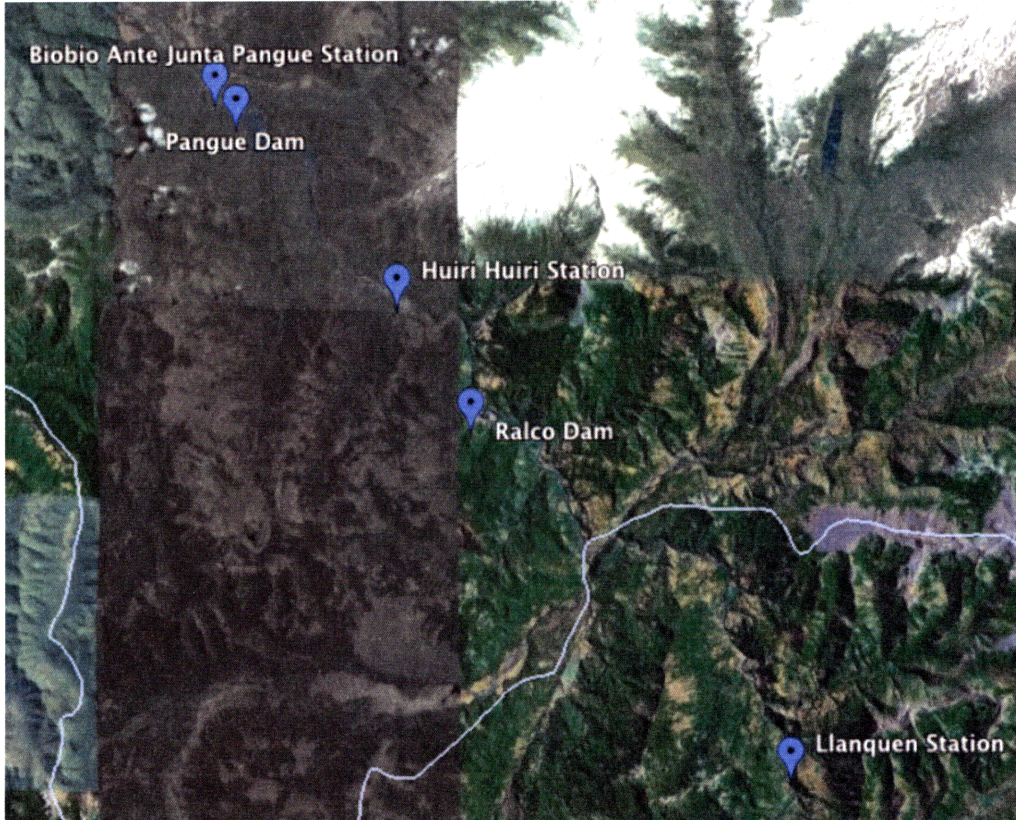


Figure 2: Satellite Image of Biobío Basin<sup>2</sup>

The upstream station, Llanquén, is shown on the lower right hand corner in the Andes mountain range. The Biobío River flows down into the Ralco reservoir, covering 3,467 hectares at full capacity (Endesa, 2009). The Ralco reservoir is not pictured in the satellite photo due to its recent creation; see Figure 1 for a graphic. From the Ralco dam, an intake draws water down about 7 kilometers to the turbines and then the restitution point,<sup>3</sup> directly upstream of the Huirí Huirí station.

Below is a schematic of the system displaying how various flows were aggregated in this model.

---

<sup>2</sup> Plotted on Google Maps (2009). UTM coordinates for flow stations obtained from MOP (2009).

<sup>3</sup> Point where the flow used to generate power is returned to the river.



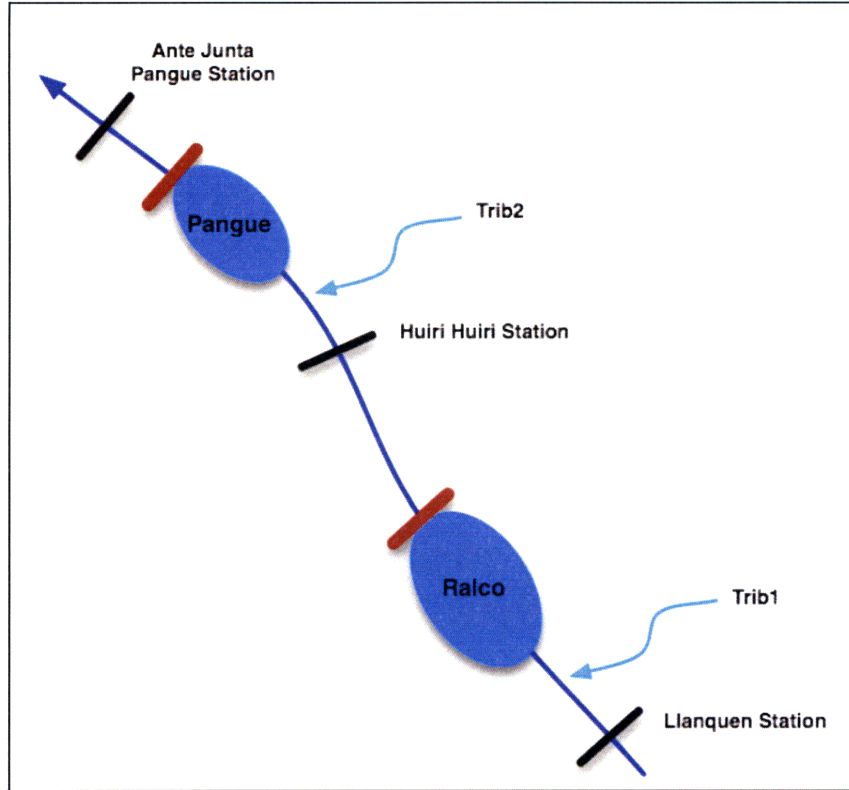


Figure 3: Schematic of Biobío Basin

Flows between Llanquén station and the Ralco dam were aggregated into the term *Trib1* and estimated with a long-term flow balance (see Appendix A.1 for details on flow series estimations). For the analysis, the upstream flow at Llanquén and the aggregated tributary flow were added together to form a single term representing inflow to the Ralco reservoir. Similarly, all tributaries between Ralco and Pangué were aggregated into the term *Trib2*. Therefore, the inflow to the Pangué reservoir included the sum of the release from the Ralco dam and *Trib2*. Measured discharges from the Ralco and Pangué reservoirs, which were used to recreate the actual release schedule, are at Huirí Huirí station (including discharge and spill) and Ante Junta Pangué station respectively.

Monthly flow series for Ralco inflow and *Trib2* were modeled as lognormal distributions with the statistical parameters of the historical data. The mean and variance for each month were calculated from the six years of data. For the replicates, each month of flow was drawn independently from a lognormal distribution with the parameters of historical data for that month of historical years. From this procedure, thirty plausible time-series for each parameter were synthesized. See Appendix A.2 for details of replicate creation.

### 2.3. Optimization Problem Formulation

The General Algebraic Modeling System (GAMS, 2008) was used to build the optimization model. In this modeling system, the objective function and all constraints are represented symbolically. GAMS uses a nonlinear solver algorithm to evaluate the optimal release schedule  $D_{i,s}$  for each reservoir and each time step (month) that optimizes the specified objective function over a horizon

of one year. In the following equation,  $Power$  generated over each month is summed over twelve months, two sites, and thirty replicates, and then normalized by the number of replicates, to represent total annual expected power output.

**Equation 1: Objective Function**

$$\max \sum_{r=1}^{30} \sum_{s=1}^2 \sum_{t=1}^{12} Power_{t,s,r} / 30$$

The optimization is subject to several constraints, the most important of which are the following.

1. **Continuity** – Water balance at each reservoir must always be satisfied. Flows considered were upstream flow, tributary flow, rainfall, evaporation from the reservoir, and outflows.

**Equation 2: General Reservoir Flow Balance**

$$S_{t+1,s,r} = S_{t,s,r} + Q_{t,s,r} - D_{t,s} - Spill_{t,s,r} + rain_{t,s} - evap_{t,s} * SA_{t,s,r} / 1e6$$

Evaporation,  $evap$ , is in meters, surface area  $SA$  is in square meters, and the factor of  $10^6$  converts cubic meters to MCM ( $10^6$  cubic meters). The indices  $t$ ,  $s$ , and  $r$  represent time step, site, and replicate number. In the general equation, the change in storage for each time step is equal to all inflows,  $Q$ , minus controlled discharge  $D$  and spilled quantity  $Spill$ , plus rainfall directly on the reservoir,  $rain$ , minus evaporative losses, in meters, multiplied by instantaneous reservoir surface area to obtain a volume. Precipitation and evaporative losses were considered to be deterministic and seasonal fluctuations were calculated from historical data for each site (see Appendix B.2).

Specific equations for Ralco and Pangué reservoirs are given below. All inflows to Ralco are included in the  $Q$  term, while inflows to the Pangué reservoir include spill and discharge from Ralco plus tributary flow in between,  $Trib2$ . Both reservoir releases include a controlled discharge term as well as a spill term.

**Equation 3: Continuity for Ralco Reservoir**

$$S_{t+1,1,r} = S_{t,1,r} + Q_{t,1,r} - D_{t,1} - Spill_{t,1,r} + rain_{t,1} - evap_{t,1} * SA_{t,1,r} / 1e6$$

**Equation 4: Continuity for Pangué Reservoir**

$$S_{t+1,2,r} = S_{t,2,r} + D_{t,1} + Spill_{t,1,r} + Trib2_{t,r} - D_{t,2} - Spill_{t,2,r} + rain_{t,2} - evap_{t,2} * SA_{t,2,r} / 1e6$$

Flows are all expressed in MCM/month ( $10^6$  cubic meters per month).

2. **Power output** – Potential power output is a function of the product of discharge ( $D$ ) and head ( $H$ ) at each time step (see Appendix C.1 for theoretical expressions). In the following expression, power  $P$  is evaluated for each time step  $t$ , each reservoir site  $s$ , and for each hydrologic time series  $r$ . Gamma ( $\gamma$ ) is a conversion factor and  $e$  is operational efficiency.

**Equation 5: Power Production**

$$P_{t,s,r} = \gamma e_s D_{t,s} H_{t,s,r} \Delta t$$

The time step,  $\Delta t$ , is expressed as hours per time period, and  $P$  is expressed in Megawatt-hours after a conversion coefficient is applied.

3. **Storage Capacity** – The storage volume in the reservoirs cannot exceed reservoir capacity.

**Equation 6: Storage Capacity Constraints**

$$\min Stor_s \leq S_{t,s,r} \leq \max Stor_s$$

Storage is constrained by the physical capacity of each reservoir in MCM,  $\max Stor$ . Minimum storage  $\min Stor$  is a constraint applied to ensure that the reservoir levels do not dip below the required operational level. For the case of Ralco, for example, water level cannot dip below the intake. Minimum storage values were estimated from documents that detailed the maximum usable storage volume for regulation as being 800 MCM for Ralco (Ingendesa, 2009) and 80 MCM for Pangué (EcoAmerica, 2009). Therefore, minimum storage levels were set at 400 MCM for Ralco and 100 MCM for Pangué.

4. **Power Capacity** – The power production cannot exceed the Megawatt rating of the turbines.

**Equation 7: Power Capacity Constraint (Major & Lenton, 1979)**

$$P_{t,s,r} \leq Y * hours * CAPH_s$$

$Y$  is the power factor, assumed here to be 1.0 for both sites, indicating this analysis does not account for demand patterns and it is assumed that all power produced over the time step can be used or stored.  $CAPH$  is the MW-rating of each plant and  $hours$  is the number of hours per time step.

5. **Maximum discharge** – Any water volume that must be evacuated each month above the maximum throughput of the turbines is considered spill and does not generate power.

**Equation 8: Maximum Throughput**

$$D_{t,s} \leq Dmax_s$$

The maximum throughput capacity  $Dmax$  for each site was determined by each site's turbine throughput rates (see Appendix B.1).

6. **Storage-Head Relationships** – Head  $H$  as a function of storage  $S$  for each site was approximated. The relationships below are quadratic fits to data (see Appendix B.1 for data source), and adjusted to reflect hydraulic head assumptions. The relationships are fitted to usable storage and are accurate for storage values greater than minimum specified storage.

**Equation 9: Ralco Storage-Head Curve**

$$H_1 = 69.4 - 5 \times 10^{-5} S_1^2 + 0.1314 S_1$$

**Equation 10: Pangué Storage-Head Curve**

$$H_2 = 28.9 - 0.002 S_2^2 + 0.7735 S_2$$

7. **Storage-Surface Area Relationships** – Linear approximations to these curves were used.

**Equation 11: Ralco Storage-SA Curve**

$$SA_1 = (S_1 - CAPD_1) * 3467e4 / CAPD_1 + 3467e4$$

The storage capacity,  $CAPD$ , for Ralco is 1,200 MCM and  $3,467 \times 10^4$  is the maximum surface area in square meters (Endesa, 2009).

**Equation 12: Pangué Storage-SA Curve**

$$SA_2 = (S_2 - CAPD_2) * 500e4 / CAPD_2 + 500e4$$

The maximum surface area for the Pangué reservoir is  $500 \times 10^4$  (EcoAmerica, 2009).

Decision variables to be determined were discharges from each dam ( $D_{i,t}$ ) that dictate storage ( $S_{i,s,r}$ ) and head ( $H_{i,s,r}$ ) in each reservoir for each replicate.

The analysis used the General Algebraic Modeling System (GAMS) and one of its nonlinear program solvers (GAMS, 2008). This problem can be formulated as a Quadratic Programming Problem (QPP) if nonlinear equality constraints are substituted into the objective function, ensuring all remaining inequality constraints are linear. See Appendix C.2 for QPP theory.

### 3. RESULTS

The optimal release schedule obtained from the GAMS model was included in two simulations to assess power gains. One simulation was run over the duration of the six-year period for which data was available. The second simulation was run over a set of 30 possible series of yearly reservoir inflows. Both simulations were run over two initial storage conditions: the first where both reservoirs were full at the start of the simulation at 1,200 MCM (Ralco) and 175 MCM (Pangué) respectively, and the second where each storage initiated at the minimum operational level specified as 400 and 100 MCM respectively.

#### 3.1. 6-Year Simulation

The 6-Year simulation used the six years of data from the DGA and compared two discharge series. The first series is a re-creation of the current scenario that utilized actual records of discharge from flow stations downstream of the reservoirs (Huirí Huirí for the Ralco reservoir and Ante Junta Pangué for the Pangué reservoir, locations of which can be seen graphically in Figure 2). The second release schedule was obtained by the GAMS optimization model and adjusted in the following way. Since the model was run over 30 potential future flow scenarios, discharge was constrained by the lowest flow month over all series. Therefore, discharge was adjusted such that if some was wasted via spill, though the discharge was still less than the throughput capacity, as much spill as possible was moved to the discharge term. The simulation forced a reduction in discharge when storage approached the minimum values. Other constraints were checked and enforced.

Below are flow and storage figures for the full initial storage condition. In the flow figures, red lines represent combined inflow (including rainfall), blue is combined outflow (including evaporation), and green is total spill volume for each reservoir.

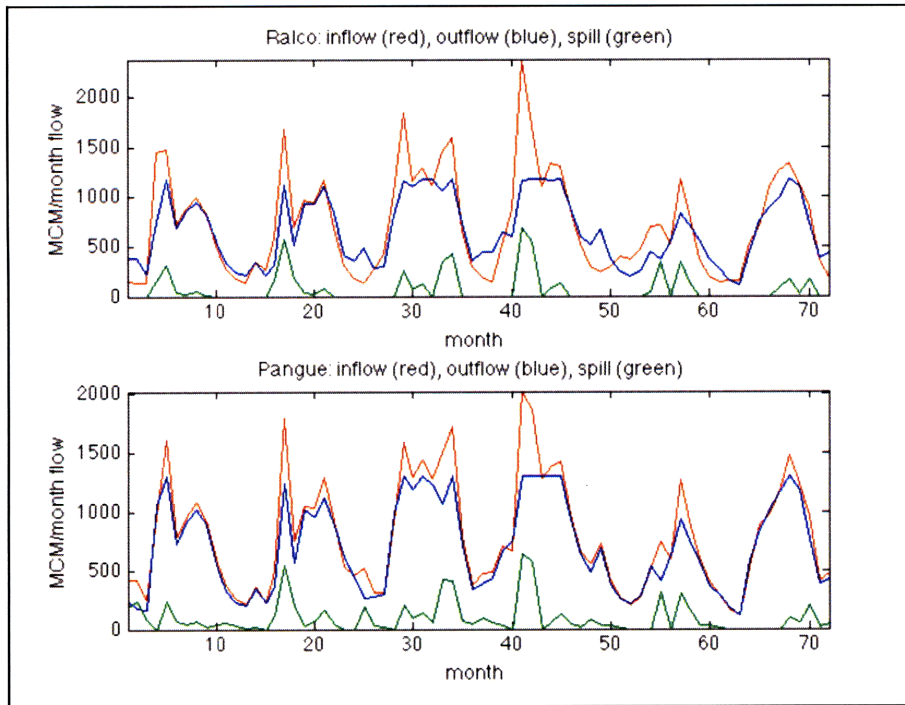


**Figure 4: Reservoir Flows, Current scenario**

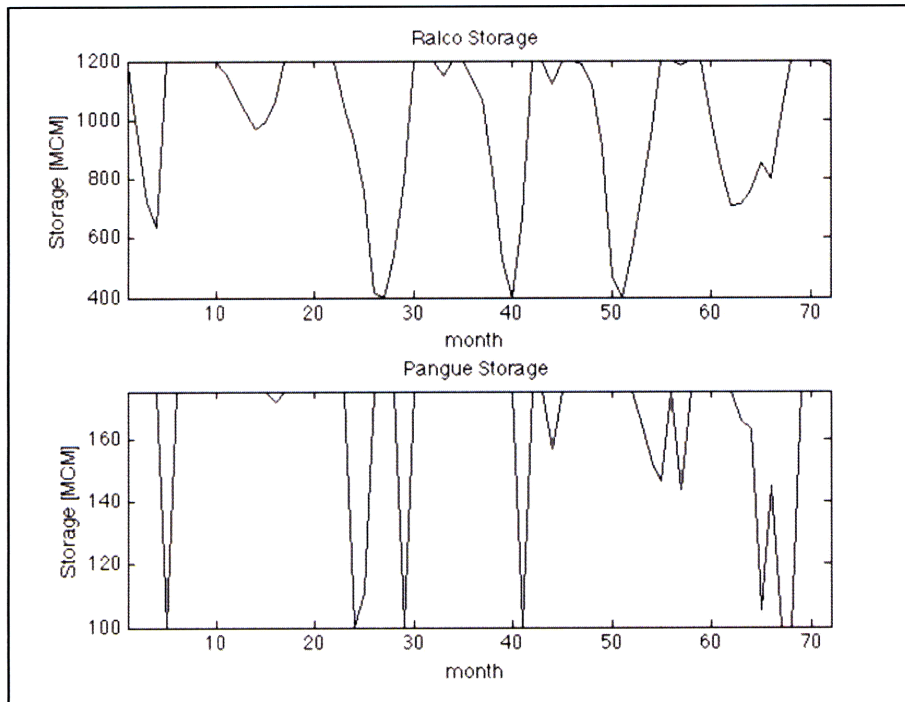


**Figure 5: Reservoir Storage, Current scenario**

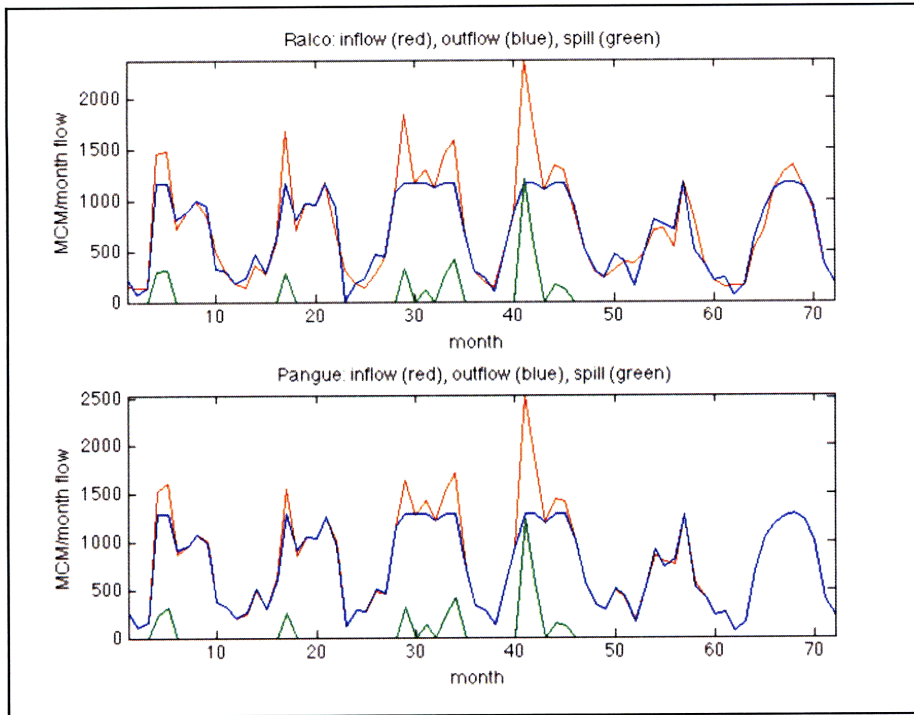


**Figure 6: Reservoir Flows, Optimal scenario**

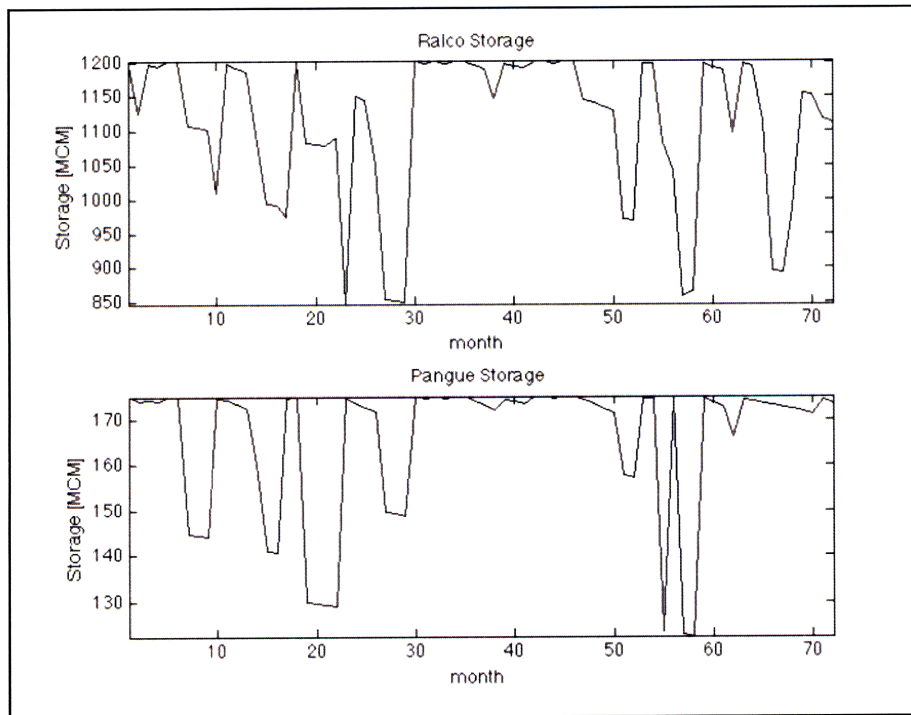


**Figure 7: Reservoir Storage, Optimal scenario**

The optimal release schedule accomplished a relatively large spill volume reduction of about **35%** for both initial storage conditions. Results for annual power production for the various scenarios and initial conditions are given in the table below.

**Table 1: 6-Year Simulation, Annual Power Production**

Initial Storage	Current, Power [GWh]		Optimal, Power [GWh]		% increase
	Ralco	Pangue	Ralco	Pangue	
Minimum	2910	2110	3090	2240	6%
Full	2960	2140	3100	2280	5%

In the 6-Year simulation, a range of **5-6% improvement** in total power generation was observed with the optimal release schedule over the recreation of the current scenario. The optimal scenario had a spill volume loss of about **7%** of the total release volume.

### 3.2. Replicate Simulation

Since this simulation used synthetic flow series, the current scenario operation rules were approximated. Average flows over the replicates for each month were assumed as the inflow series, and the operation rule was to release the expected inflow for the month if storage was full or close to full, and a reduced amount if storage approached the minimum. Flows were adjusted to ensure constraints were not violated.

The current operating scheme for this simulation is not intended as an approximation to how the reservoirs would actually be operated given the replicate flow series. It simply displays an operation rule that could be used to form a basis for comparison to the optimized scenario. The table below summarizes annual power production results from the simulation.

**Table 2: Replicate Simulation, Annual Power Production**

Initial Storage	Current, Power [GWh]		Optimal, Power [GWh]		% increase
	Ralco	Pangue	Ralco	Pangue	
Minimum	2560	1970	2880	2140	11%
Full	2990	2240	3090	2290	3%

In the Replicates simulation, a range of **3-11%** improvement was observed with the optimal release schedule over the simple operation rule. Spill losses from the optimal scenario represented about **5%** of total discharge volume.

### 3.3. Conclusions

Total current hydropower production in Chile is about 20,000 GWh/year (EIA, 2008). The Biobío case study can be extrapolated to the remaining hydropower systems, assuming the systems have similar potential for improved operations and spill reduction. With these assumptions, potential gain from operations (3-11%) is estimated to be between **600 and 2,200 GWh/year** over all hydropower systems in Chile. The high end is an upper bound obtained from the comparison of the simple

operating rule to the optimal release series, as the optimal scenario achieves 5-6% power gains over the re-creation of the actual scenario over six years. While not insignificant, this amount does not replace the need for new power projects. Additionally, the potential gain from spill reduction from the optimal scenario is another 5-7% by volume. To glean as much as possible from current hydropower systems, the following areas for improvement can be investigated.

1. **Operations** – Stochastic optimization formulation can be improved with longer series of historical data. Also, if it is possible to accurately predict flows within a short time frame, a real-time control system with a flow forecasting input (from weather predictions) can be utilized to reduce waste due to spill.

The efficacy of this technique depends on the upper bound for total potential gain from a perfect prediction of future flows. In this case, running a deterministic optimization over all 30 replicates showed that the added potential power production from perfectly forecasting the future ranges from 0 to 8% with a mean of 3% over the optimal scenario developed in this analysis. This gain corresponds to 0 to 15% with a mean of 6% over the simple operating rule defined in the replicate simulation. This means that, given perfect information about future flows, the optimal operating procedure would only gain an **average of 6%** over a simple operating rule. The small potential gain suggests that spending such time and effort in the development of a real-time control model is probably not necessary for this system.

However, it is possible that more accurately characterizing historical variability could yield more years where the high end of 15% power gains could be obtained. The possibility of achieving power gains closer to the high end of the range indicates the potential benefit from a real-time control model. For this system, with more data, and for other systems, a similar analysis should be completed to evaluate the effectiveness of a real-time control system.

If the potential gain from a good forecast is high for a given multi-dam hydropower system, a stochastic Model Predictive Control (MPC) technique could be used to formulate the real-time control model. A forecast of future flows, along with current state variables such as storage volume, is input into a stochastic optimization over a specified time interval. The first optimal control decision is implemented for the current time step. At the next time step, the process is repeated with new state information and new forecasts. See Appendix C.4 for MPC details.

2. **Increased reservoir storage** – Storage would have to be significantly increased and doing so would flood additional area and likely incur environmental and social detriment. Potential gains for different reservoir sizes should be assessed prior to construction as storage is probably not feasible to adjust in an already operational hydropower dam.
3. **Increased hydraulic head** – Since power is proportional to the product of hydraulic head and discharge, an obvious way to increase power production is to increase the height of the dam. In many cases such a post-construction modification is infeasible, however, in some cases it is possible to increase height by a couple of meters with technology like fuse gates. This technique requires flooding additional area.
4. **Increased turbine throughput capacity** – This can be accomplished by replacing turbines



with higher throughput models or by adding more turbines. Such alterations are probably logistically infeasible in an operational facility, as large modifications to the turbine housing structure and probably the intake as well would be necessary. In order to capture the power from high flow events observed in the simulations of the Biobío case study, about a **50% increase** in throughput capacity would be required. A detailed cost-benefit analysis would be necessary to evaluate potential gains from harnessing high flow events compared to extra cost of higher throughput capacity. Such an analysis is likely to be most useful if completed prior to construction.

From these simulations, it appears that current operations of the hydropower systems on the Biobío River are harnessing very close to the maximum amount of power. Only very small gains can be expected through further optimizing operations, and it is possible these gains are only seen because of the various assumptions that were required due to lack of information. The potential gains for various optimization techniques, such as real-time control with forecasting, should be assessed for other large hydropower systems in Chile.

Depending on the hydropower system, gains can likely be achieved by a combination of improved release schedules, use of weather forecasting in a real-time control model, and prior evaluation of the optimal throughput capacity and reservoir characteristics.

## APPENDIX A. METHODS DETAIL

### A.1. DATA ANALYSIS

Daily data was obtained for all required stations (Llanquén, Ante Junta Pangué, and Huirí Huirí) for the longest contiguous period of time available. This study analyzed six years of daily data for all stations between 1/2003 and 1/2009 from the DGA (2009).

Daily data was converted into monthly average data, ignoring gaps if possible. Monthly averages were assessed ignoring data gaps by simply calculating an average over available data. If necessary, data gaps were filled in with values interpolated linearly from days surrounding missing data.

All inflows between Ralco and Pangué were aggregated into the term *Trib2*. Inflow between Llanquén and Ralco was termed *Trib1*, which included all tributaries downstream of the Llanquén station as well as those that feed directly into the reservoir.

*Trib2* was estimated by assuming that, over a long period of time (the six-year period between 2003 and 2009), the total tributary flow should equal the difference between the Ante Junta Pangué and Huirí Huirí. That is equivalent to assuming constant storage in the Pangué reservoir over the six years. The tributary flow was subsequently distributed as Huirí Huirí's flows over the year such that the seasonal variation follows Huirí Huirí but sums to the appropriate amount. However, it is likely that storage was increasing over that time period and thus *Trib2* was underestimated. The final paragraph of this section describes an adjustment made to remedy this possibility.

*Trib1* was estimated by a similar process, which assumed the Ralco reservoir started and ended at relatively constant volume over the six-year period. The tributary flow was then distributed monthly as scaled by the Llanquén station flows.

Finally, tributary flows were adjusted for *Trib1* and *Trib2* such that during the current operation scenario (when flow station Huirí Huirí was assumed to be the outflow from Ralco and Ante Junta Pangué station the outflow from Pangué), the storage in each reservoir did not dip below the minimum storage prescribed as 400 MCM for Ralco and 100 MCM for Pangué. The amount required to prevent storage from dipping below the minimum values was added to the estimated tributary flow.

### A.2. REPLICATE CREATION

Data from stations upstream and downstream of each reservoir were aggregated into monthly flow series. From the flow stations and a long-term water balance, direct inflows to the reservoirs were estimated.

The top left figure of Figure 8, below, shows the six years of aggregated inflow to the Ralco reservoir. The other three figures show synthesized replicates. In each figure, 10 of 30 replicates are shown. Aggregated inflow to Ralco includes the sum of Llanquén and *Trib1*. The following figure, Figure 9, shows the yearly data and replicates for *Trib2*.

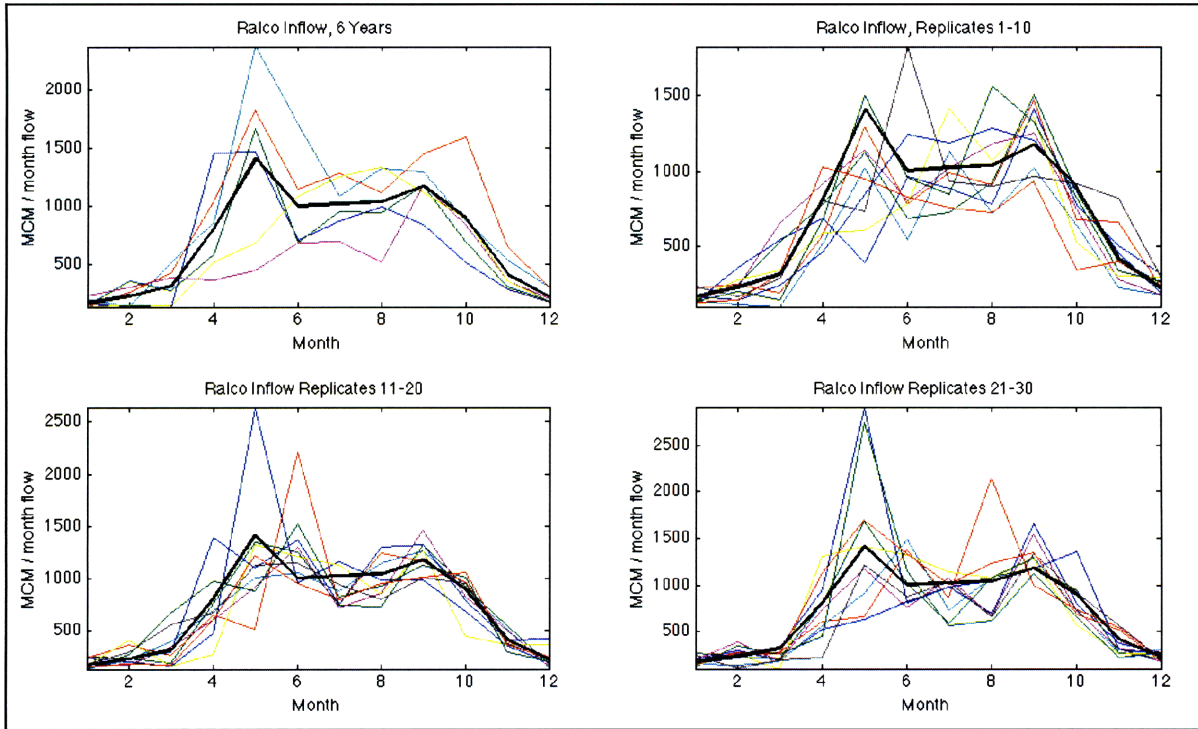


**Figure 8: Historical Data and Synthesized Time-Series for Ralco Inflow**

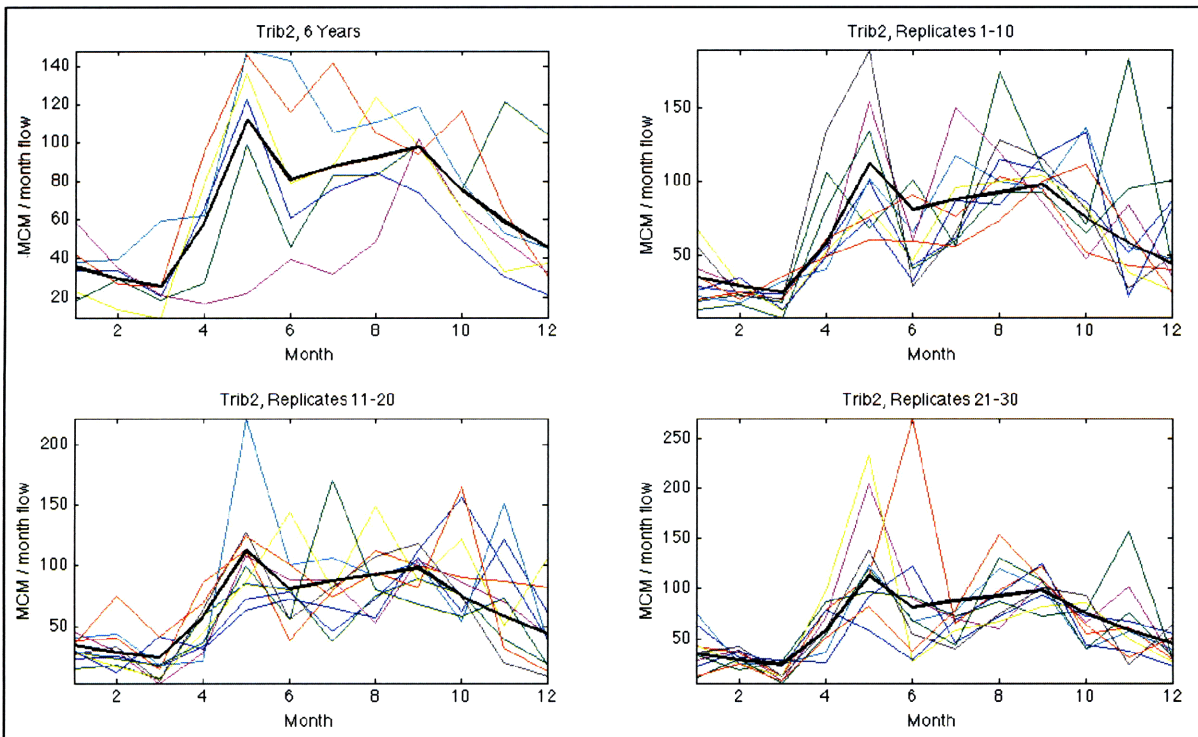


**Figure 9: Historical Data and Synthesized Time-Series for Trib2**

Seasonal variability is well represented in these replicates, as are peaks and lows. Of course, additional historical data would be useful in better characterizing potential future series.

Replicates were generated assuming the flow in each month, month  $i$ , is lognormally distributed with mean and variance equal to the historical mean and variance for month  $i$  over the 6-year period. Thirty replicates were generated for each of two flow series (aggregated inflow to Ralco and Trib2) in a matrix using MATLAB's **lognrnd** function. The parameters can be calculated as (MATLAB, 2009):

$$\begin{aligned}\mu &= \log(m^2 / \sqrt{v + m^2}) \\ \sigma &= \sqrt{\log(v / m^2 + 1)}\end{aligned}$$

Where  $m$  and  $v$  are the mean and variance of the historical data.

## APPENDIX B. ASSUMPTIONS

### B.1. DAM AND RESERVOIR CHARACTERISTICS

#### Reservoir Geometry

- **Maximum surface area**
  - Ralco: 3,467 hectares at full storage (Endesa, 2009)
  - Pangué: 500 hectares at full storage (EcoAmerica, 2009)
- **Storage**
  - Maximum: 1,200 MCM for Ralco and 175 MCM for Pangué
  - Minimum: There is reason to believe the storage is not allowed to dip below the prescribed values of 400 MCM and 100 MCM for Ralco and Pangué respectively; this is because the “live” or usable storage for each is approximately 800 MCM (Editec, 2009) and 80 MCM respectively (EcoAmerica, 2009).
- **Hydraulic Head**
  - Ralco: Estimated hydraulic head is 155m when the reservoir is full. This is an approximation based on observed power performance, since exact specifications for the height of the intake and the total drop to the turbines could not be found. There appears to be a larger head difference than 155m but there is head loss in the long length of pipe, so it was decided that hydraulic head would be back calculated using power production with a full reservoir (690 MW operating at full throughput capacity of 450 m<sup>3</sup>/s corresponds to a hydraulic head of about 155m).
  - Pangué: Hydraulic head was approximated as height of water at the dam, with a maximum of 103m (Université du Québec à Montréal, 2009). Unfortunately, this analysis lacks crucial dam specifications that would be found in the inaccessible EIA.
- **Storage-Head relationships**
  - Quadratic curves were fitted to data obtained from a university course project (Brown & Vargas, 2004).
- **Storage-Surface area** curves approximated linearly using maximum surface area corresponding to a full reservoir.
- **Maximum throughput (*D<sub>max</sub>*):** 450 m<sup>3</sup>/s for Ralco (Editec, 2009) and 500 m<sup>3</sup>/s for Pangué (EcoAmerica, 2009).
- **Minimum spill** was not considered. Ralco is required to spill a minimum ecological flow to maintain water in the river between the dam and the restitution point but it is not accounted for in this analysis.

#### Power Production

- **Efficiency** was estimated as the discrepancy between theoretical power capacities based on

the maximum hydraulic head and maximum throughput and the MW-rating of each plant.

- **MW Capacity** of Ralco is assumed to be 690 MW (Editec, 2009) and Pangué to be 467 MW (Colegio de Ingenieros de Chile, 2009)
- **Power factor** (or load factor) is assumed to be 1.0, meaning demand patterns are not considered. It is assumed that power produced at any time can be utilized.

## B.2. EVAPORATION AND PRECIPITATION

Precipitation and evaporation are not modeled stochastically. Each is estimated to vary in the same way over each year according to historical trends for each site.

### Precipitation

Precipitation in meters was estimated as having the seasonal variation of a precipitation curve shown in a DGA report for 2004 (DGA, 2004). For each site, the total precipitation expected per year was scaled by the seasonal variation curve. Approximate yearly values in millimeters were obtained from the same DGA report. Ralco, in the upper part of the Biobío basin, was approximated to have 3,000 mm per year total precipitation, concentrated between May and August.

Precipitation volume was estimated as the amount falling on the entire reservoir area, irrespective of the current storage level, assuming all rainfall within that region ends up in the reservoir. Approximated precipitation volumes for the Ralco reservoir are shown in Figure 10.

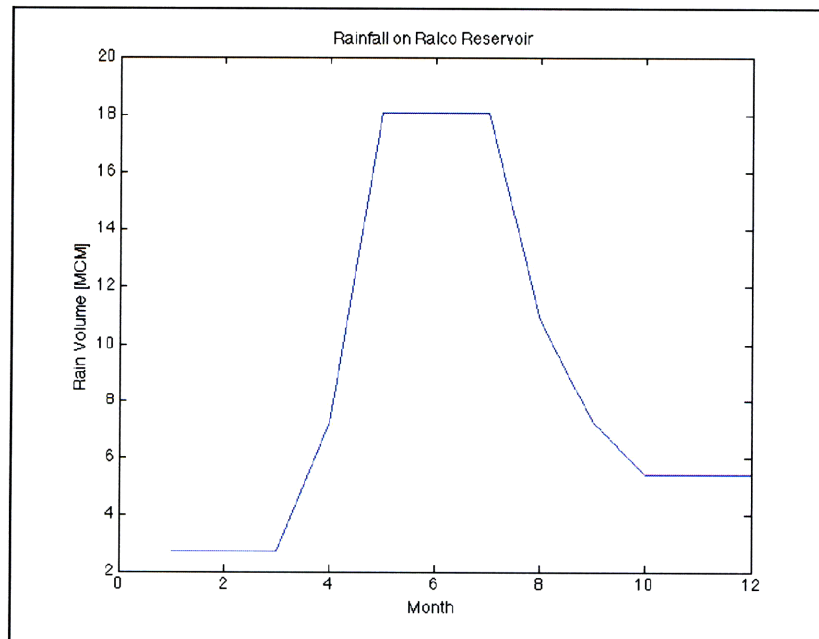


Figure 10: Approximated Rainfall on the Ralco reservoir

Pangué, located between Ralco and Los Angeles, was approximated to have 2,000 mm/year precipitation with the same seasonal variation.

## Evaporation

Ralco was assumed to have a total of 101.6 mm/month<sup>4</sup> and Pangué to have 122.2 mm/month in evaporative losses. In order to obtain the seasonal variation, it was assumed evaporation is roughly twice as high in the summer months as the rest of the year.

---

<sup>4</sup> According to the report (translated): “As for water losses from evaporation product in the basin average monthly values reached 122.2 mm in the area of Los Angeles. In parts High River Bío Bío (Ralco), evaporation is lower, reaching values of 101.6 mm/year.” (DGA, 2004). This analysis has assumed that the 101.6 mm/year is a mistake and really intends the value to be per **month**.

## APPENDIX C. LITERATURE REVIEW

### C.1. Hydroelectric Power Production

Hydroelectric plants use water turbines to drive generators that produce electrical power. The hydropower production function is proportional to the product of discharge through the turbines and hydraulic head at the dam, described by the following equation:

**Equation 13: Hydroelectric Power Generation**

$$P = E \int R(t)H(t)dt$$

Where  $P$  is power,  $R(t)$  is the rate of water discharge, and  $H(t)$  is the instantaneous hydraulic head at the dam.  $E$  is a constant based on the efficiency and load factor of the plant (Mays, 1996 as referenced by Chatterjee, et al., 1998). When time is discretized, the total power production can be written as follows (Major & Lenton, 1979):

**Equation 14: Discretized Power Production**

$$P_i = \gamma e R_i H_i \Delta t$$

Where  $P_i$  [MWh] is the power production over time step  $i$ ,  $R_i$  is the total discharge over the period,  $H_i$  is head at the beginning of the period (or an average head over the period),  $\Delta t$  is the number of hours in the period, and  $\gamma$  is a conversion coefficient. The unitless constant  $e$  represents the operating efficiency of the plant.  $H$  is a function of  $S$ , the total storage in reservoir  $s$  at the beginning of time period  $t$ , as determined by the geometry of the reservoir.

### C.2. Quadratic Programming Theory

This optimization model is described by a quadratic objective function and linear constraints, and the technique that such solves a problem is termed Quadratic Programming.

The basic theory behind solving quadratic programming problems, in the general case, will be outlined below. The mathematical problem formulation is the following (McLaughlin, 2008):

$$\underset{x_1, x_2, \dots, x_n}{\text{Maximize}} F = c_j x_j + \frac{1}{2} x_j Q_{jk} x_k \rightarrow \underset{x}{\text{Maximize}} F(x) = c^T x + x^T Q x$$

such that

$$g_i(x) = A_{ij} x_j - b_i \leq 0, \quad i = 1, \dots, m_T$$

$$g_i(x) = -x_i \leq 0, \quad i = m_{T+1}, \dots, m_{T+n}$$

or

$$g(x) = G^T x - \beta \leq 0$$

where



$$G^T = \begin{bmatrix} A \\ -I \end{bmatrix}, \beta = \begin{bmatrix} b \\ 0 \end{bmatrix}$$

$$Dim(G) = (n)X(m_T + n), Dim(\beta) = (m_T + n)X(1).$$

$Q$  is a symmetric matrix.  $G_i$  are the constraint inequalities. There may also be equality constraints, but generally those can simply be used to eliminate a decision variable until the problem can be constrained solely by inequalities.

Define the following expressions:

- $C(x)$ : set of constraints active at solution  $\mathbf{x}$  (includes active inequalities and strict equalities)
- $\widehat{G}_\mu(x)$ :  $\mathbf{n}$  by  $m_A$  active gradient matrix at  $\mathbf{x}$ , comprised of columns of  $G_{j_i}$  with  $i \in C(x)$
- $\widehat{\beta}_i(x)$ :  $\mathbf{n}$  vector of active right-hand side values at  $\mathbf{x}$ , comprised of rows of  $\beta_i$  with  $i \in C(x)$
- $\widehat{Z}_\mu(x)$ :  $\mathbf{n}$  by  $n - m_A$  active constraint tangent matrix (the columns are orthogonal to columns of  $\widehat{G}$  such that  $\widehat{G}^T(x)Z(x) = 0$ )
- $\widehat{G}^T x - \beta = 0$ : active constraint equations

The argument  $\mathbf{x}$  may be eliminated in the following discussion for clarity, though it should be noted which of the above matrices are dependent on the current solution  $\mathbf{x}$ .

### C.2.1. Local and Global Optimality of a QPP

#### Local Optimality

In order for a candidate solution  $\mathbf{x}^*$  to be locally optimal, the Kuhn-Tucker conditions need to be satisfied. The Kuhn-Tucker conditions ensure that  $\mathbf{x}^*$  is a local maximum by checking that  $F(x^*) \geq F(x)$  for all  $\mathbf{x}$  obtained from **infinitesimal feasible perturbations** about  $\mathbf{x}^*$ . The following discussion will include the basic application of the Kuhn-Tucker conditions to a QPP. The four basic conditions, as applied to a QPP, are as follows (McLaughlin, 2008):

1. **Feasibility** – Solution  $\mathbf{x}^*$  is feasible if and only if  $\widehat{G}^T x^* - \beta \leq 0$ , meaning all constraints are satisfied.
2. **Stationarity** – The objective function gradient at  $\mathbf{x}^*$  must be a linear combination of the  $m_A$  active constraint gradient vectors. Using the definition of the objective function for a QPP,

$$\widehat{G}^T \lambda = \frac{\partial F(x^*)}{\partial x} \rightarrow \widehat{G}^T \lambda = c + Qx^*$$

Each component of  $\lambda$ ,  $\lambda_i$ , is the Lagrange multiplier for the associated constraint  $g_i(x)$ . Stationarity is satisfied if the above set of linear equations is consistent, or

$$\rho = Rank[\widehat{G}] = Rank[\widehat{G} | c + Qx^*].$$

3. **Inequality Lagrange Multipliers** – If  $\mathbf{x}^*$  is a local maximum,  $\lambda_i \geq 0$  for all active inequalities.
4. **Curvature** – Feasible perturbations of  $\mathbf{x}^*$  must lie in the active constraint tangent subspace

defined by  $Z_{j_l}(x^*)$ . The curvature of the objective function in the active constraint tangent subspace is measured by the projected Lagrangian Hessian matrix  $W_{lk}$ ,

$$W_{lk} = Z^T \frac{\partial^2 L(x^*, \lambda)}{\partial x \partial x} Z = \frac{\partial^2 L(x^*, \lambda)}{\partial x_j \partial x_q} Z_{j_l} Z_{q_k}. \text{ If } x^* \text{ is a local maximum, } \mathbb{W} \text{ must be negative semidefinite, meaning that the eigenvalues of } \mathbb{W} \text{ are } \leq 0. \text{ For a QPP, } W_{lk} = \tilde{Z}_{k_l}(x^*) Q_{jk} \tilde{Z}_{j_l}(x^*) \leq 0 \text{ is the necessary condition.}$$

If  $x^*$  satisfies all four Kuhn-Tucker conditions, it is a local maximum.

### Global Optimality

Once a candidate solution  $x^*$  has been proven to be a local optimum, it is necessary to check if it is also a global optimum. The necessary conditions are twofold:

1. The feasible region is convex. For a QPP, the feasible region is always convex since it is comprised of linear constraints, which are both convex and concave.
2. The objective function is concave along feasible perturbations from all  $x \in F$ , the feasible region. Thus, the projected Hessian used in KT condition 4 must be negative semidefinite for all points in the feasible region including boundaries (not just at  $x^*$  as confirmed in KT4):  $\tilde{Z}^T(x) Q \tilde{Z}(x) \leq 0$  for all  $x \in F$ .

For a QPP, if the above expression is satisfied, a local maximum is a global maximum.

A QPP optimization must be solved once for a single optimization, as in this analysis, or at every time step in a real-time control procedure. The procedure for finding the optimal solution (carried out by many commercial software packages) can be any number of methods including interior point, active set, or conjugate gradient methods. Generally, active set methods are utilized.

### C.3. Other Stochastic Optimization Methods

Unknown hydrologic variables are always a challenge in water resources optimization. In a reservoir system, upstream inflows are generally the variable in question. Techniques such as Stochastic Dynamic Programming (SDP) have been widely used in such problems to account for inflow uncertainty in the sequential stages of the decision process. In SDP models developed between the 1960s and the 1980s, inflows were often described as a Markov chain process. Such methods, known as ‘steady-state’ SDP optimization, were traditionally used to generate stationary policies, which dictate optimal releases for a given system state (storage and previous inflow) at a given time (Serrat-Capdevila & Valdes, 2007). A minimum expected cost is also defined for each state of the system. More recently, real-time SDP formulations have been proposed by authors such as Bras *et al.* (1983) and Alarcon and Marks (1979). In real-time methods, expected costs associated with each state of the system are used as boundary conditions for the optimization over a finite horizon, and the process is repeated at each time step.

In deterministic SDP, a multi-stage problem is solved by optimizing a recursive equation, starting from the final stage and following a backward recursion. At each stage, the decision variable is optimized depending on the state of the system. If the state of the system is known (as in the deterministic case), this can be done directly; when the inflow is considered as a random variable, the decision is based on weighing each possible inflow with its probability of occurrence as determined by all historical records available. Effective representation of stochastic variables

depends on how decision variables are assigned based on previous hydrologic data and estimated probability distributions for the future time steps. Thus, it is important to derive realistic distributions for stochastic variables, which requires each time step's flows to be discretized into ranges, each of which is assigned a probability of occurrence (Bras *et al.*, 1983, Tejada-Guibert *et al.*, 1995, and Capdevila & Valdes, 2006). For example, one approach would discretize time into  $n$  stages, flow into  $n$  ranges, and would require the use of  $n$  transition probability matrices.

A steady-state formulation would dictate operating policies for each time step of one water-year depending on the state of the system (current storage and previous inflow). The inflows would be modeled as annual periodic first order Markov chains (Serrat-Capdevila & Valdes, 2007) from which current stage probabilities could be derived, each conditional upon previous stage inflow. Such a steady-state formulation would assume constant probability distributions for each year. Autoregressive forecasting dictates that if the previous stage inflow deviated from the historical mean, the expected values for subsequent stage flows will deviate in the same direction, given a historical positive correlation between future stage flows (Serrat-Capdevila & Valdes, 2007).

Stochastic Model Predictive Control techniques have been discussed by authors Calafiore *et al.* (2000), Khargoneka and Tikku (1996), Stengel and Ray (1993), Tempo and Bai (1997), Tempo and Dabbene (1999) as referenced in Batina (2004).

#### **C.4. Model Predictive Control**

In order to evaluate the optimal solution to a real-time control problem, a technique called Model Predictive Control (MPC) can be employed. MPC is an algorithm that uses a dynamic model of the process, a history of control decisions, and an optimization cost function over the prediction horizon to calculate the next set of optimum control decisions (Bemporad *et al.*, 2001). The time-step is determined by the scale of volatility of the inputs and the time resolution of flow forecasting.

The steps involved in an MPC analysis are as follows:

- Assume future time series for inputs for the remaining planning horizon (using flow predictions based on weather patterns for the duration of additional knowledge from forecasting, then historical data for times past prediction range)
- Adjust operations by solving the optimization problem at the current time-step using known current values of inputs. Optimize decision variables over all times in the planning horizon with the all assumed future input series.

At each time-step, MPC solves a single optimization problem. Given the current state of the system (storage, head, and inflow), the amount of water to be released from each dam at each time-step over the rest of the planning horizon is determined. Using this procedure, real-time decisions about reservoir operating schemes can be made at each specified time-step.

#### **Theory**

MPC is a real-time optimization method by which a set of optimum control moves is developed at each time-step for the rest of the planning horizon. MPC is analogous in many ways to strategy games such as chess. In chess, a skillful player envisions a sequence of likely moves for his opponent and chooses his first move based on the sequence that optimizes the expected end result.

Only one move can be applied before the opponent chooses a move, which may or may not be what the first player predicted. Thus, the vector of future opponent moves is like the vectors of unknown input variables. Such a strategy is termed a “receding horizon” algorithm since at each time-step, the finite planning horizon to be optimized is shifted by one frame into the future. The methodology of MPC can be described as follows (Camacho & Bordons, 1999).

1. At each instant  $t$ , all future input series to the model are predicted over the planning horizon  $N$ . The predicted series depend on all known values (inputs and outputs) prior to instant  $t$  as well as on the future control signals  $u_{i+1}$ ,  $i = t \dots N-1$ .
2. The future control signals over the rest of the planning horizon  $N$  are calculated. This set includes values  $u_t \dots u_{T-1}$ . In traditional MPC, this is done by minimizing a cost function that is a quadratic representation of the error between the predicted output signal and a reference trajectory. However, in this model, a quadratic benefit function representing net monetary gain from hydropower production will be maximized over the planning horizon.
3. The first control signal  $u_t$ , the control action for the current time, is implemented. All future control signals are discarded since the entire vector of values will be recalculated in the following time step based on new state and input variable values. Step 1 is then repeated using the new state and input values for step  $t + 1$  and all future control decisions for the shortened and shifted horizon  $N$ ,  $u_{t+1} \dots u_{T-1}$ , are determined (Huang & Kadali, 2008).

The MPC process is well described graphically.

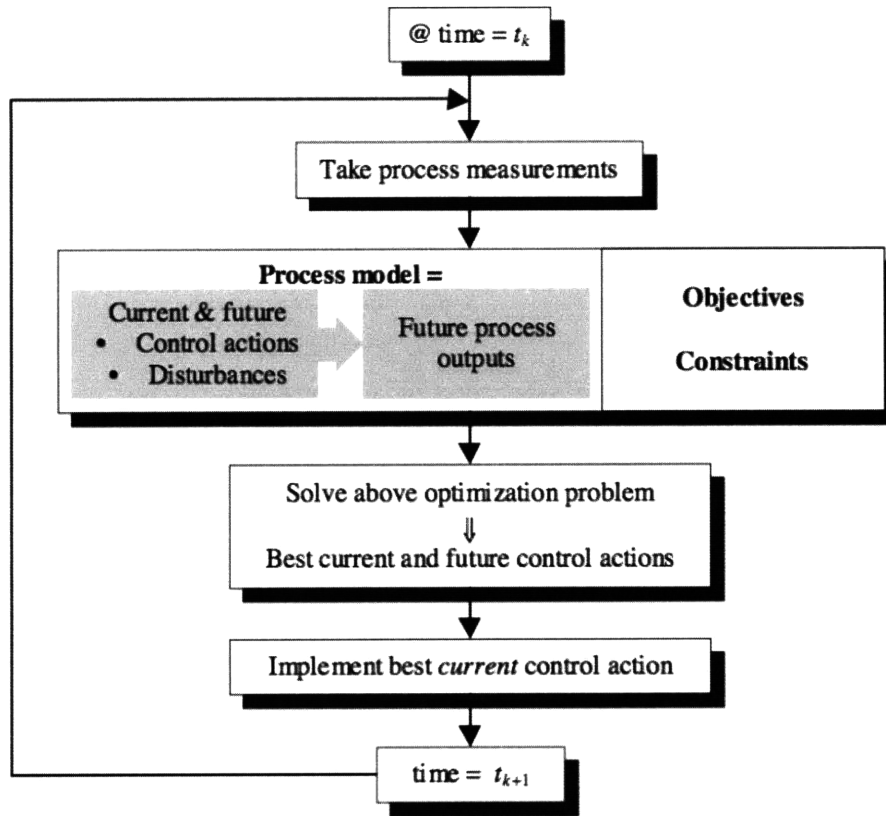


Figure 11: Model Predictive Control Schematic (Nikolaou, 2001)

At each time  $t_k$ , process measurements are taken and fed into a prediction of future inputs, which is used in conjunction with the process model to optimize control signals over the rest of the planning horizon. At each time step, only the first control move is implemented, and the entire optimization problem is resolved considering a new measurement of input and state variables.

In this case, the control signals are represented by a matrix of the discharges from each reservoir for the rest of the planning horizon, starting with the current time  $t$ :

$$\begin{bmatrix} u_i^{s=1} & u_i^{s=2} \\ \vdots & \vdots \\ u_{T-1}^{s=1} & u_{T-1}^{s=2} \end{bmatrix} = \begin{bmatrix} R_i^{s=1} & R_i^{s=2} \\ \vdots & \vdots \\ R_{T-1}^{s=1} & R_{T-1}^{s=2} \end{bmatrix}, i = t \dots T-1$$

The “state” of the system is a matrix including the current storage  $V_i$  and the previous stage inflow,  $Q_{i-1}$ , for each of two reservoirs.

## APPENDIX D. REFERENCES

- Alarcon, L., & Marks, D. (1979). *A stochastic dynamic programming model for the operation of the High Aswan dam*. Technical Report 246, Ralph M. Parsons Lab., Department of Civil Engineering, Massachusetts Institute of Technology, Cambridge, MA
- Arnold, E., Tatjewski, P., Wolochowicz, P. (1994). Two methods for large-scale nonlinear optimization and their comparison on a case study of hydropower optimization. *Journal of Optimization Theory and Applications*, 81(2), 221-248.
- Batina, I. (2004). Model predictive control for stochastic systems by randomized algorithms. (PhD, Technische Universiteit Eindhoven).
- Bemporad, A., Borrelli, F., & Morari, M. (2000). The explicit solution of constrained LP-based receding horizon control. *Decision and Control, 2000. Proceedings of the 39th IEEE Conference on*, 1, 632-637 vol.1.
- Bemporad, A., Borrelli, F., & Morari, M. (2001). Model Predictive Control Based on Linear Programming – the Explicit Solution. Technical Report AUT01-06, Automatic Control Laboratory, Dip. Ingegneria dell'Informazione, Università di Siena, Zurich, Switzerland
- Biao Huang, Ramesh Kadali. (2008). Model predictive control: Conventional approach. *Dynamic modeling, predictive control and performance monitoring A data-driven subspace approach*, 101-119. Retrieved from Springer Berlin / Heidelberg. doi:10.1007/978-1-84800-233-3
- Bras, R. L., Buchanan, R., & Curry, K. C. (1983). Real time adaptive closed loop control of reservoirs with the High Aswan Dam as a case study. *Water Resources Research*, 19(1), 33-33-52.
- Brown, E., & Vargas, X. CI71C Análisis Hidrológico y Evaluación de Recursos Hídricos. (2004). Retrieved Mar. 11 2009 from [https://www.ucursos.cl/ingenieria/2004/1/CI71C/1/material\\_docente/objeto/](https://www.ucursos.cl/ingenieria/2004/1/CI71C/1/material_docente/objeto/)
- Cai, X., McKinney, D., & Lasdon, L. (2001). Solving nonlinear water management models using a combined genetic algorithm and linear programming approach. *Advances in Water Resources*, 24(6), 667-676.
- Calafiore, G. C., Dabbene, F., & Tempo, R. (2000). Randomized algorithms for probabilistic robustness with real and complex structured uncertainty. *IEEE Transactions on Automatic Control*, 45(12).
- Chatterjee, B., Howitt, R. E., Sexton, R. J. (1998). The optimal joint provision of water for irrigation and hydropower. *Journal of Environmental Economics and Management*, 36, 295-313.
- CIA (Central Intelligence Agency). (2008). Chile. *The World Factbook*. Retrieved November 30, 2008 from <https://www.cia.gov/library/publications/the-world-factbook/geos/ci.html>
- Colegio de Ingenieros de Chile A.G. *Desafíos Eléctricos y Grandes Obras de los Últimos Cincuenta Años*. Retrieved March 3, 2009 from [www.ingenieros.cl/index.php?option=com\\_docman&task=doc\\_download&gid=435&Itemid=](http://www.ingenieros.cl/index.php?option=com_docman&task=doc_download&gid=435&Itemid=)
- CONAMA. Estudio de Impacto Ambiental: "Proyecto Central Hidroeléctrica Angostura." Retrieved March 5, 2009 from <https://www.e->

seia.cl/expediente/expedientes.php?modo=ficha&id\_expediente=3142073&idexpediente=3142073

- D.C. Major, L. Lenton. (1979). The mathematical programming screening model. *Applied Water Resource Systems Planning* (pp. 59-59-81). Englewood Cliffs, NJ: Prentice-Hall.
- Derechos Human Rights. *Ralco: Represa o pobreza?* 1 June 2002. Retrieved February 13, 2009 from <http://www.derechos.org/nizkor/chile/libros/endesa/cap2.html#E1%20Proyecto%20de%20la%20Central%20Hidroel%20ctrica%20de%20Ralco>
- DGA (Dirección General de Aguas). (2004). *Diagnostico y Clasificacion de los Cursos y Cuerpos de Agua Segun Objetivos de Calidad, Cuenca del Rio Bio Bio*. Retrieved March 5, 2009 from [http://www.sinia.cl/1292/articles-31018\\_Biobio.pdf](http://www.sinia.cl/1292/articles-31018_Biobio.pdf)
- DGA (Dirección General de Aguas). (2009). *Servicios Satelitales en Tiempo Real*. Retrieved March 1, 2009 from <http://dgasatel.moptt.cl/>
- EcoAmerica. Informe de la comision investigadora sobre presuntas irregularidades en la apertura de las compuertas de la Central Pangué. Retrieved March 1, 2009 from [http://www.ecoamerica.cl/sitio/upload/241/1169216198\\_informe%20pangué.doc](http://www.ecoamerica.cl/sitio/upload/241/1169216198_informe%20pangué.doc)
- Ediciones Especiales. *Ralco por dentro: Un retrato intimo*. Retrieved April 5, 2009 from [http://www.edicionesespeciales.elmercurio.com/pdfs/File\\_20040927115324.pdf](http://www.edicionesespeciales.elmercurio.com/pdfs/File_20040927115324.pdf)
- Editec. *Central Ralco Radiografía de la hidroeléctrica*. Retrieved February 21, 2009 from <http://www.editec.cl/electricidad/Elec77/articulos/ralco.htm>
- Eduardo F. Camacho, Carlos Bordons. (2007). Nonlinear model predictive control: An introductory review. *Assessment and future directions of nonlinear model predictive control*.
- EIA (Energy Information Administration). (2008). *Chile Energy Profile*. Official Energy Statistics from the United States Government. Retrieved 1 December 2008 from [http://tonto.eia.doe.gov/country/country\\_energy\\_data.cfm?fips=CI](http://tonto.eia.doe.gov/country/country_energy_data.cfm?fips=CI)
- El-Awar, F. A., Labadie, J. W., & Oarda, T. B. M. J. (1998). Stochastic differential dynamic programming for multi-reservoir control. *Stochastic Hydrology and Hydraulics*, 12, 247-266.
- Endesa. *Ralco Hydro Plant (Chile) Begins to Operate with 120 MW More Capacity than Forecast*. Rep. Retrieved February 20, 2009 from <http://www.scepc.net/NR/rdonlyres/er6jhs06fmocy7xkezwyxidencwctsnvacomecz3osbc22iuvy2m7cki2ftuivcho6r7swdl52t7g/PotenciaRalcoing.pdf>
- General Algebraic Modeling System (GAMS). Retrieved December 1, 2008 from <http://www.gams.com/>
- GENI (Global Energy Network Institute). (2002). *An Energy Overview of Chile*. Retrieved November 29, 2008 from [http://www.geni.org/globalenergy/library/national\\_energy\\_grid/chile/EnergyOverviewofChile.shtml](http://www.geni.org/globalenergy/library/national_energy_grid/chile/EnergyOverviewofChile.shtml)
- Gonzalez, J. A., & Nabona, N. (2000). Multicommodity long-term hydrogeneration optimization with capacity and energy constraints. *Sociedad De Estadística e Investigación Operativa Top*, 8(1), 73-96.
- Google. *Google Maps*. Retrieved February 15, 2009 from <http://maps.google.com>

- Graf, W.L. (1999). Dam nation: A geographic census of American dams and their large-scale hydrologic impacts. *Water Resource Research* 35(4): 1305–1311.
- Grancharova, A., Johansen, T. A. (2005). Survey of explicit approaches to constrained optimal control. *Switching and Learning in Feedback Systems*, 47-97. Retrieved from Springer Berlin / Heidelberg. doi:10.1007/b105497
- Ilich, N. (2001). The benefits of replacing LP solvers in basin allocation models with a generalized nonlinear evolutionary network flow solver. *World Water and Environmental Resources Congress*, Reston, VA.
- Ingendesa. *Características del Diseño y Construcción de la Presa Ralco en Chile*. Rep. Retrieved February 9, 2009 from <http://www.ingendesa.cl/images/publicaciones/CaracteristicasPresaRalco.pdf>
- International Rivers. (2008). *Patagonia*. Retrieved 15 November 2008 from <http://internationalrivers.org/en/latin-america/patagonia>
- Khargonekar, P. P., & Tikku, A. (1996). Randomized algorithms for robust control analysis and synthesis have polynomial complexity. Paper presented at the *Conference on Decision and Control*, Kobe, Japan. 3470-3475.
- Li, X., & Wei, X. (2008). An improved genetic algorithm-simulated annealing hybrid algorithm for the optimization of multiple reservoirs. *Water Resources Management*, 22, 1031-1031-1049. doi:DOI 10.1007/s11269-007-9209-5
- Love, J. (2007). Model predictive control. *Process automation handbook*, 1023-1038. Springer London. doi:10.1007/978-1-84628-282-9
- Luhandjula, M., & Gupta, M. (1996). On fuzzy stochastic optimization. *Fuzzy Sets Systems*, 81, 47-47-55.
- Maeder, U., Cagienard, R., Morari, M. (2007). Explicit model predictive control. *Advanced strategies in control systems with input and output constraints*, 237-271. Retrieved from Springer Berlin / Heidelberg. doi:10.1007/978-3-540-37010-9
- MATLAB (The MathWorks - MATLAB and Simulink for Technical Computing). *Statistics Toolbox - Documentation*. Retrieved April 1, 2009 from <http://www.mathworks.com/access/helpdesk/help/toolbox/stats/index.html?/access/helpdesk/help/toolbox/stats/lognrnd.html&http://www.google.com/search?client=safari&rls=en-us&q=lognormal+distribution+matlab&ic=UTF-8&oe=UTF-8>
- Mays, L. W. (1996). *Water resources handbook*. New York: McGraw-Hill.
- McLaughlin, D. (2008). *1.731: Water Resource Systems Lecture Notes. Lectures 6-10*. Unpublished manuscript.
- Ministerio de Obras Públicas (MOP). *Alerta Hidrológica*. Retrieved Feb. 16, 2009, from <http://www.mop.cl/dga-WebModule/alertaAction.do?op=2>
- Nation Master Encyclopedia (2005). *Aysén Region*. Retrieved November 30, 2008 from <http://www.nationmaster.com/encyclopedia/Aysén-Region>
- Nikolaou, M. (2001). *Model predictive controllers: A critical synthesis of theory and industrial needs*. Unpublished. University of Houston, Houston, TX.



- Otero, J., Labadie, J., Haunert, D. (1995). Optimization of managed runoff to the st. lucie estuary. Paper presented at the *First International Conference, Water Resources Engineering Division, ASCE, San Antonio*.
- Pabich, W. J. (2008). Request for Proposal. Massachusetts Institute of Technology, Department of Civil and Environmental Engineering.
- Raman H. C. (1996). Deriving a general operating policy for reservoirs using neural network. *Journal of Water Resources Planning and Management*, 122(5), 342-342-347.
- Ray, L. R., & Stengel, R. F. (1993). A monte carlo approach to the analysis of control systems robustness. *Automatica*, 3, 229-236.
- Serrat-Capdevila, A., & Valdes, J. B. (2007). An alternative approach to the operation of multinational reservoir systems: Application to the Amistad & Falcon system (lower Rio Grande/Rio Bravo). *Water Resources Management*, 21, 677-698. doi:DOI 10.1007/s11269-006-9035-1
- Sharif, M., & Wardlaw, R. (2000). Multireservoir systems optimization using genetic algorithms: Case study. *Journal of Computing in Civil Engineering*, 14(4), 255-255-263.
- Stengel, R. F., & Ray, L. R. (1991). Stochastic robustness analysis: Explicit bounds for the minimum number of samples. *IEEE Transaction on Automatic Control*, 36, 82-87.
- Tatjewski, P. (2007). Model-based predictive control. *Advanced control of industrial processes* () Springer London. doi:10.1007/978-1-84628-635-3
- Tejada-Guibert, J., Johnson, S., & Stedinger, J. R. (1995). The vale of hydrologic information in stochastic dynamic programming models of a multi-reservoir system. *Water Resources Research*, 31(10), 2571-2579.
- Tempo, R., & Dabbene, F. (1999). Probabilistic robustness analysis and design of uncertain systems. In G. Picci, D. S. Gilliam (Ed.), *Dynamical systems and control, coding and computer vision*, Birkhauser.
- Tempo, R., Bai, E. W., & Dabbene, F. (1997). Probabilistic robustness analysis: Explicit bounds for the minimum number samples. *System and Control Letters*, 30, 237-242.
- Université du Québec à Montréal. Retrieved March 2, 2009 from [www.er.uqam.ca/nobel/r34670/narratives/Pangue\\_s.txt](http://www.er.uqam.ca/nobel/r34670/narratives/Pangue_s.txt)
- Zhang, J. L., & Ponnambalam, K. (2006). Hydro energy management optimization in a deregulated electricity market. *Optim Eng*, 7, 47-61. doi:DOI 10.1007/s11081-006-6590-5